Micro Acoustic Resonant Chambers for Heating/Agitating/Mixing (MARCHAM)

Stewart Sherrit, Aaron C. Noel, Anita M. Fisher, Nobuyuki Takano, Frank Grunthaner
Jet Propulsion Laboratory, California Institute of Technology, Pasadena, CA

Abstract – A variety of applications require the mixing and/or heating of a slurry made from a powder/fluid mixture. One of these applications, Sub Critical Water Extraction (SCWE), is a process where water and an environmental powder sample (sieved soil, drill cuttings, etc.) are heated in a sealed chamber to temperatures greater than 200 degrees Celsius by allowing the pressure to increase, but without reaching the critical point of water. At these temperatures, the ability of water to extract organics from solid particulate increases drastically. This paper describes the modeling and experimentation on the use of an acoustic resonant chamber which is part of an amino acid detection instrument called Astrobionibbler [Noell et al. 2014, 2015]. In this instrument we use acoustics to excite a fluid- solid fines mixture in different frequency/Amplitude regimes to accomplish a variety of sample processing tasks. Driving the acoustic resonant chamber at lower frequencies can create circulation patterns in the fluid and mixes the liquid and fines, while driving the chamber at higher frequencies one can agitate the fluid and powder and create a suspension. If one then drives the chamber at high amplitude at resonance heating of the slurry occurs. In the mixing and agitating cell the particle levitation force depends on the relative densities and compressibility's of the particulate and fluid and on the kinetic and potential energy densities associated with the velocity and pressure fields [Glynne-Jones, Boltryk and Hill 2012] in the cell. When heating, the piezoelectric transducer and chamber is driven at high power in resonance where the solid/fines region is modelled as acoustic transmission line with a large loss component. In this regime, heat is pumped into the solution/fines mixture and rapidly heats the sample. We have modeled the piezoelectric transducer/chamber/ sample using Mason's equivalent circuit. In order to assess the validity of the model we have built and tested a variety of chambers. This paper describes the experimental results which are in general agreement with theory within the limitations of the modeling.

Keywords: Piezoelectric vibration, heating, fluid particle interaction, Subcritical water extraction

Introduction

A major thrust of space exploration is to answer the important astrobiology question about the viability of life elsewhere in the universe [De Marais et al. 2003]. Answering this question using robotic missions is extremely challenging due to the mass, volume and power limitations imposed on spacecraft. It is not enough to measure a concentration of organic chemicals associated with life on another planetary body. Nature can produce a large variety of molecules found in living cells (prebiotic chemistry) [Miller 1953]. For example natural processes produce over 75 amino acids while amino acids associated with life is only a small subset of these (20 or more). The organic chemistry produced by nonliving process generally produce distributions that are broadly defined and racemic (have equal amounts of left- and right-handed enantiomers of a chiral molecule). Extinct life displays a mixture of racemic and homochiral distributions (enantiomeric) while extant life shows selective distributions of the 20 or so amino acids and they are decisively homochiral. The determination of the chirality of a chemical species is one analytical method to search for life on other worlds as specific chirality is strongly associated with molecules produce by living organisms. Organics produced by extant and extinct lifeforms have a preferential chirality which mixed with prebiotic chemistry produce an enantiomeric mixture. In order to confirm if the organic chemical was produced by an extant or extinct life form from a chemical measurement one must measure the chemical species distribution and the chirality to determine if there is a preferential chirality. The relationship between these chemical properties and life are shown in Figure 1.

The Astrobionibbler task is a micro fluidic soil amino acid detector that can be used to detect amino acids using laser induced fluorescence and as a front end instrument to extract and concentrate amino acids for downstream instrumentation. The microfluidic instrument is composed of four major components 1/ Mixing chamber where the soil sample is mixed and agitated with the solvent (water). 2/ Subcritical water extraction chamber where the sample is heated to > 200ºC and up to 1.6 MPa pressure. 3/Filter or settling chamber. 4/ An H-cell with a Laminar Flow Diffusion Interface (LFDI) to allow amino acids to flow across and interact with a fluorophore. The measurement is

done using a laser beam which is scanned across the LFDI. The amino acid combines with fluorescamine to form a fluorophore which can be excited by the laser light. Since there is a one to one chemical relationship between the amino acid and fluorescamine the intensity of the fluorescence is a measure of the amino acid concentration. If the diffusion coefficients of the fluorophore are much less than the amino acids one could recirculate both channels of the H-cell until all the amino acids have been extracted from the sample solution and concentrated in the fluorophore solution. A schematic of the Astrobionibbler system is shown in Figure 2. The first step in this determination is the process of extraction of the organic material from a rock powder or soil sample [Saim et al. 1997, Hawthorne et al. 2000, Ramos, Kristenson, Brinkman 2002].

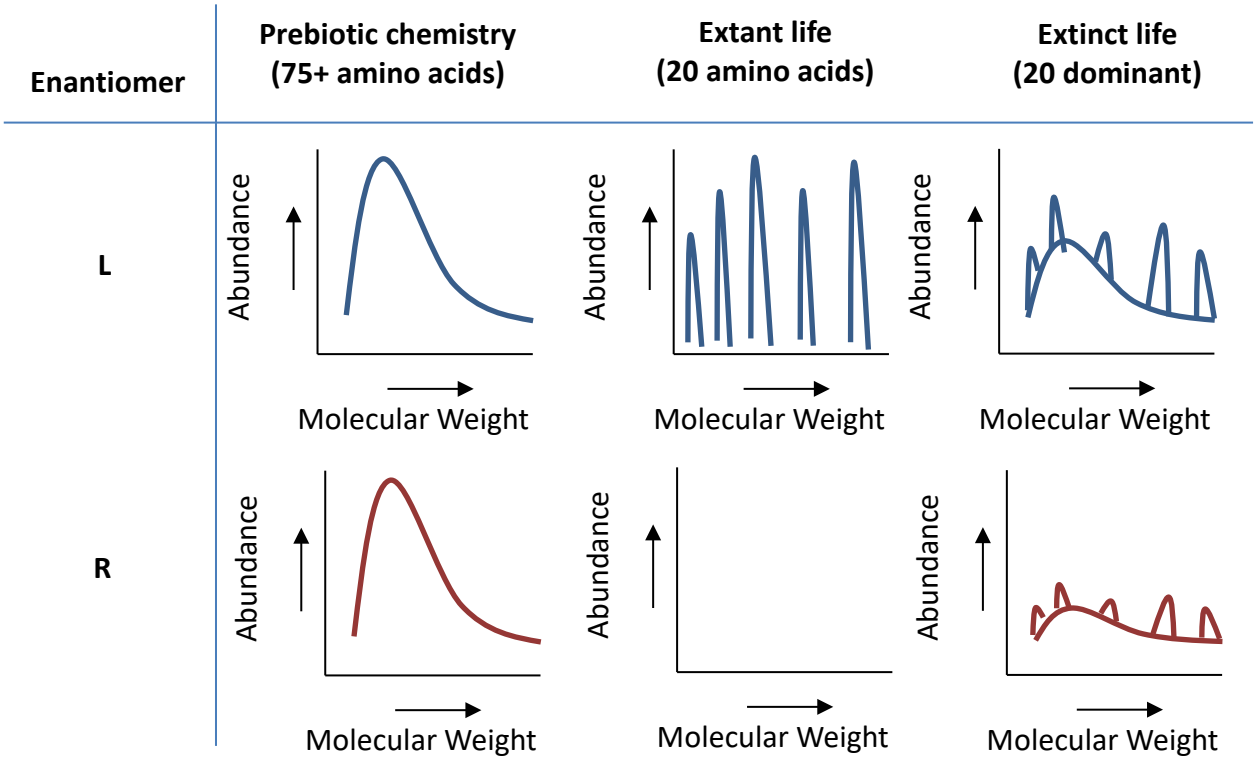

Figure 1: Schematic explanation of the relationship between chirality and extinct and extant life with different sample types and their associated spectra.

As noted in the above references there are a variety of ways to extract organics from solid phase materials including; Pressurized liquid extraction (PLE) [Benthin, Danz, Hamburger 1999, Carabias-Martínez et al. 2005], supercritical water extraction (SPE)[Yanik et al. 1995], subcritical and supercritical CO_2 extraction (SCCDE, SPCCDE), [Hamdan et al. 2007], and Subcritical Water Extraction (SCWE) [Yang et al. 1995, Liang, Amashukeli et al. 2007 and Fan 2013]. Subcritical water extraction is a form of PLE however with the use of water as the solvent. The polarity, viscosity, surface tension, and disassociation constant of sub-critical water are significantly lowered as the temperature of water is increased [Liang and Fan 2013] above its atmospheric boiling point of 100˚C while the diffusivity and the self-ionization are found to increase [Chaplin et al. 2015]. In this state water becomes a better solvent due to the reduction of the dielectric constant which mimics other low dielectric constant solvents. To maintain superheated or subcritical water requires that the chamber be held at under pressure (Pressure must be greater than the vapor pressure at the solvent temperature. Subcritical water can exist between temperatures or 100 ºC and 374 ºC where the water becomes supercritical [Liang and Fan 2013]. This papers describes an acoustic method of heating and agitating the slurry on a microfluidic chip using an ultrasonic piezoelectric transducer. The theory and experimental results for a variety of designs of SCWE cells are presented.

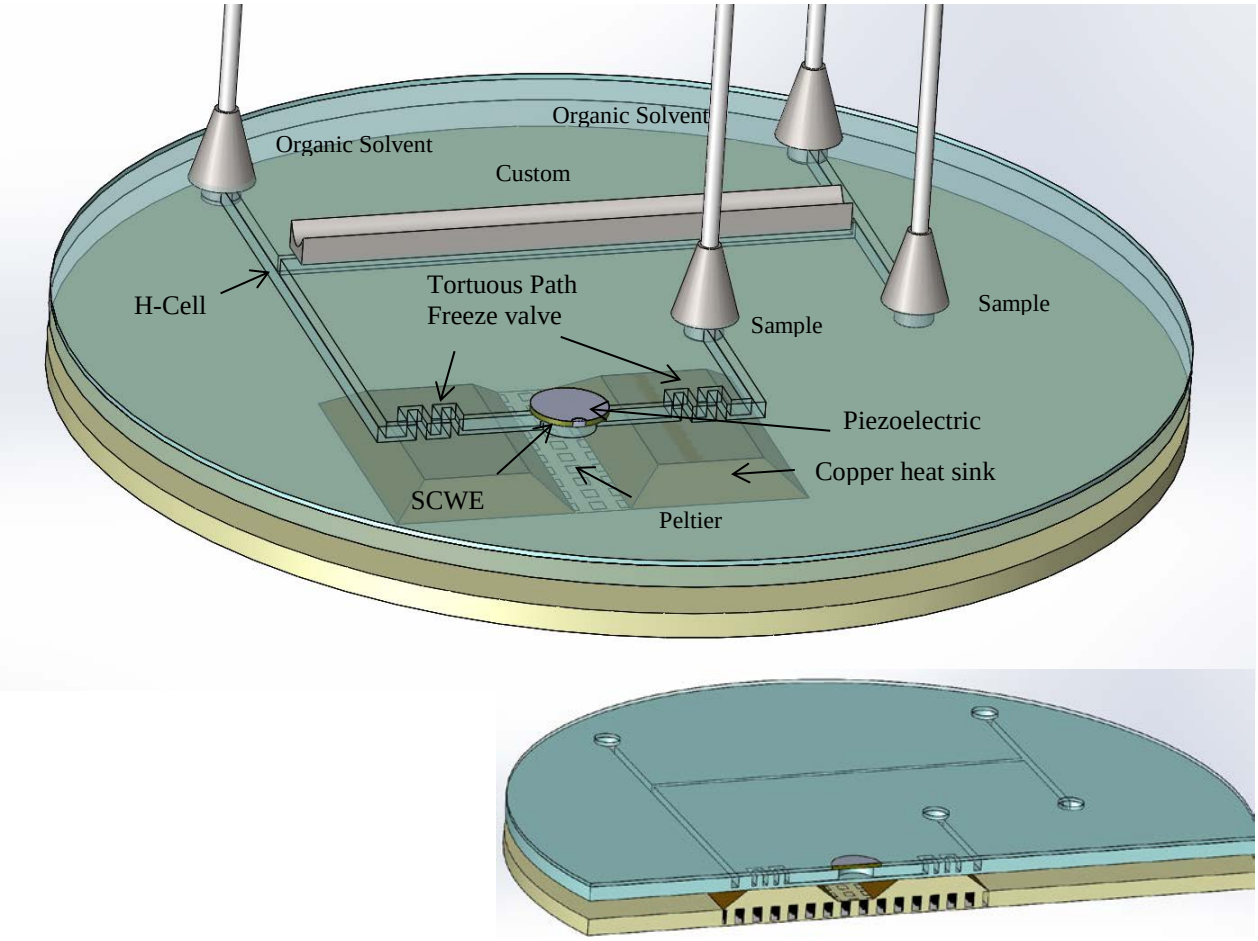

Figure 2: Schematic view of the Astrobionibbler instrument concept. The sealing of the SCWE chamber is done via freeze valves activated by Peltier coolers. The Laminar Flow Diffusion Interface (LFDI) is beneath the optional custom lens. A cross section shows the Peltier coolers that are used to freeze the inlet and outlet channels of the SCWE. The mixing and agitating and settling or filtering is done off chip.

Theory of the Acoustic SCWE

The use of acoustics in microfluidic devices to manipulate suspended particles in fluids has been known for a very long time and interest in the technology over the last decade has renewed due to advances in microfluidics and MEMs [King, 1934, Yosioka, and Kawasima 1955, Bao et al. 2009, Bruus et al. 2011]. In designing systems to manipulate suspended particles the emphasis is on generating the acoustic streaming forces while minimizing the acoustic loss [Hahn and Dual 2015]. In the Acoustic SCWE the emphasis is on heating and the piezoelectric transducer is driven at field levels where non-linear effects in the dielectric, and mechanical loss may be dominant. Unfortunately analytical models for non-linear piezoelectrics have only seen limited development. One way of handling this is to treat the material coefficients as field dependent and to adjust the magnitude the loss factors accordingly. In this study we have used linear network theory and have adjusted the material coefficients to reflect the deficits in the models. These models are expected only to guide the development and may under extreme drive levels have limited fidelity in accurately describing the heat generation mechanism. For example we know that the heating of the SCWE chamber is from both mechanical heating in the fluid due to attenuation and conduction from the dielectric heating in the piezoelectric. In the modeling presented in this paper we will model simplified geometries of the SCWE (water chamber diameter and piezoelectric diameter are matched) and then extend the model to our design geometries.

The acoustic velocity in a material depends on the stiffness and the density of the medium. In addition as acoustic waves travels through a medium they are attenuated due to scattering, porosity, inhomogeniety, and density

variations etc. Attenuation in Newtonian liquids is primarily controled by the viscosity. The relationship between the viscosicty and the attenuation α in a newtonian fluid is

$$\alpha = \frac{2\left(\eta+\frac{4}{3}\eta^{V}\right)\omega^{2}}{3\rho V^{3}} \quad (1)$$

Where η is the dynamic viscosity and η^V is the bulk or volume viscosity , ρ the density, ω is the sound frequency and V is the sound velocity. This is a baseline attenuation. In a slurry, where there are particles of higher density and acoustic velocity the attenuation is increased due to scattering from the particulate and this can a dominant source of the attenuation. Recent studies by [Hahn and Dual 2015] looked at the various attenuation processes in acoustic microfluidic devices and found that the attenuation due to viscous damping at the cavity walls due to the no-slip condition was by far the most severe of all the damping mechanisms they studied including scattering.

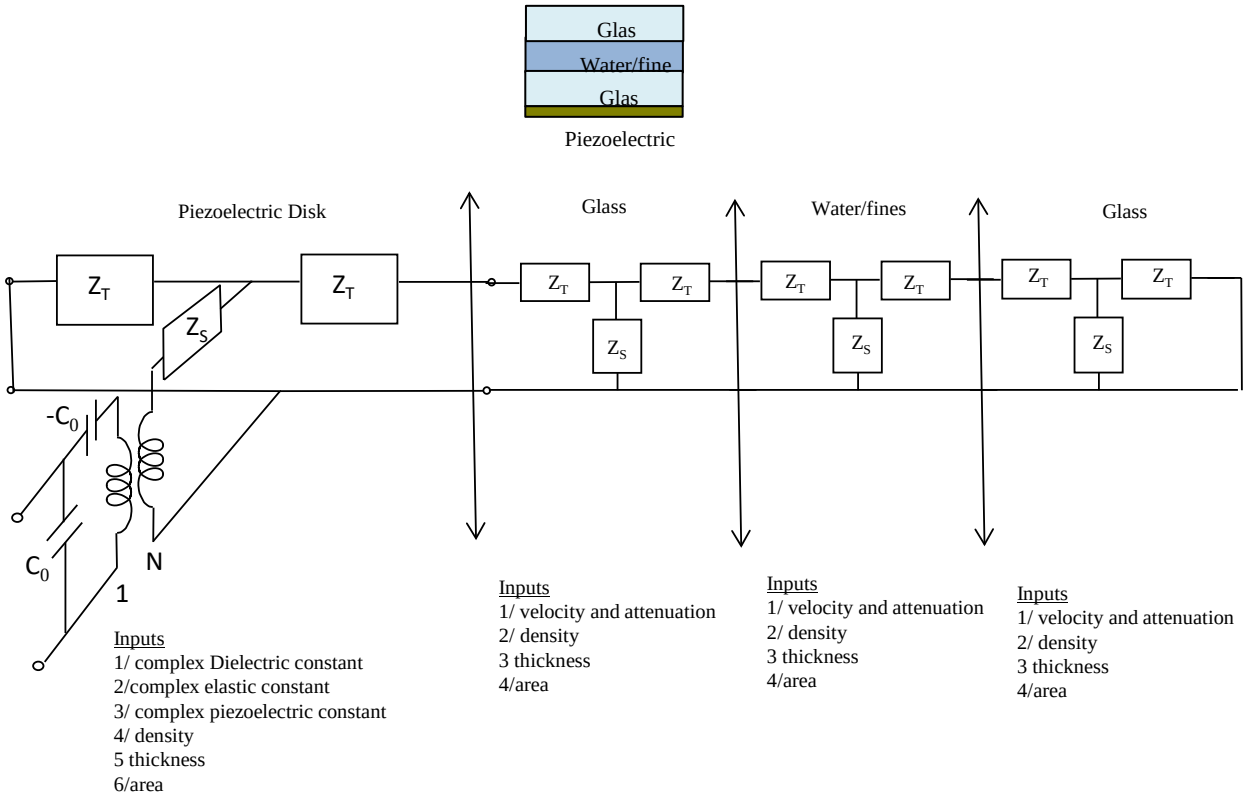

Figure 3: A schematic representation of the Acoustic SCWE model along with the Mason's equivalent network representation. The shematic shows the piezoelectric on the chip from bottom to top of the microfluidic chip while the network model is from left to right.

In order to model the acoustic subcritical water extraction we use Mason's network model [Mason 1948, 1958, Berlincourt Curran and Jaffe 1964, Sherrit et al. 1999] to calculate the ultrasonic power dissipated in the various layers in the model. A schemaitc of the physical model is shown in Figure 3 along with the network equivalent circuit. The 1D model has 4 acoustic layers. The piezoelectric disk can be modeled using the network equivalent circuit on the left which uses an ideal transformer to transfer the electrical variables voltage V, Current I to the velcity v and the force F. The circuit on the right of the transformer behaves in the similar manner as an electrical circuit however the current is a one to one transform to velocity and the voltage V transforms to the force F. The circuit to the left of a transformer is fully electrical. Every acoustic layer is treated with as a T network with $Z_T = i\rho vAtan(\omega t/2v)$ and $Z_S = -i\rho vAcsc(\omega t/v)$ where i = $\sqrt{-1}$, ρ is the density of the layer and t the layer thickess, A is the layer area and v is the complex velocity (velocity and attenuation). Due to the low density and velocity of air we asssume the surface is stress free which is modeled with a short on the left and right termination accoustic ports. On a terminating impedance as is found the glass layer on the right the parallel combination $Z_T + Z_TZ_S/(Z_T+Z_S)$is found to be $Z_{TT} = i\rho vAtan(\omega t/v)$. The equations for the variables in Mason's equivalent circuit are shown in Table 1. In the thickness mode the variables that are used to model the piezoelectric are the clamped permitivity

$\boldsymbol{\varepsilon}_{33}^{S}$, the open circuit elastic stiffness $\mathbf{c}_{33}^{D}$ and complex electromechanical coupling constant $\boldsymbol{k}_t$. The equations for the static capacitance C_o and the impedance Z_o and the turns ratio **N** are shown in the table along with relationships of the piezoelectric coefficients $\mathbf{e}_{33}$ and $\mathbf{h}_{33}$. The piezoelectric properties and the Mason's equivalent circuit parameters are shown in Table 2.

Table 1. The relationship between the complex material constants and the parameters of Mason's equivalent circuit.

$\boldsymbol{\varepsilon}_{33}^{S}$ clamped complex permittivity
$\mathbf{c}_{33}^{D}$ open circuit complex elastic stiffness
$\boldsymbol{k}_t$ complex electromechanical coupling
$\boldsymbol{k}_t^2 = \boldsymbol{e}_{33}^2 \big/ \mathbf{c}_{33}^{D}\boldsymbol{\varepsilon}_{33}^{S} = \boldsymbol{h}_{33}^2\boldsymbol{\varepsilon}_{33}^{S} \big/ \mathbf{c}_{33}^{D}$
$\boldsymbol{h}_{33} = \boldsymbol{k}_t\sqrt{\mathbf{c}_{33}^{D} / \boldsymbol{\varepsilon}_{33}^{S}}$
Mason's Model
$\mathbf{C}_0 = \frac{\boldsymbol{\varepsilon}_{33}^{S} A}{t}$ $\qquad$ $\mathbf{N} = \mathbf{C}_0\boldsymbol{h}_{33}$
$\boldsymbol{Z}_0 = \rho\, A\mathbf{v}^{D} = A\sqrt{\rho\, \mathbf{c}_{33}^{D}}$ $\qquad$ $\boldsymbol{\Gamma} = \frac{\omega}{\mathbf{v}^{D}} = \omega\sqrt{\frac{\rho}{\boldsymbol{c}_{33}^{D}}}$
$Z_T = i\mathbf{Z}_0 \tan(\boldsymbol{\Gamma} t/2)$ $\qquad$ $Z_S = -i\mathbf{Z}_0 \csc(\boldsymbol{\Gamma} t)$

Table 2. The complex material constants and the parameters of Mason's equivalent circuit for the piezoelectric disk used in these studies (APC Nebulizer disk # 50-1014).

ρ = 7700 kg/m^3 $\quad$ t = 0.00123 m $\quad$ Diameter = 0.0138 m
$\mathbf{c}_{33}^{D}$ (x 10^{11} N/m^2) = 1.62 (1 + 0.00957i)
$\boldsymbol{\varepsilon}_{33}^{S}$ (x 10^{-9} F/m) = 8.49(1 - 0.04i)
$\boldsymbol{h}_{33}$ (x 10^{9} V/m) = 2.02 (1 + 0.023i)
$\boldsymbol{k}_t$ = 0.462 (1 - 0.00194i)
$\mathbf{C}_0$ (nF) = 1.03 (1 – 0.04i)
N (C/m) = 2.08 (1 - 0.017i)
$\mathbf{v}_D$ (m/s) = 4583 (1 + 0.0048i)

The complex material coefficients were determined from the impedance resonance of the bare piezoelectric and are shown in Figure 4. The points are the data and the line is the fit to the data using the coefficients shown in Table 2. The resonance is very noisey with many sideband resonances which is likely due to the radial- thickness coupling. The resonance frequency is about 1.65 MHz while the anti resonance frequency is 1.85 MHz. The acoustic properties of the layers are shown in Table 3. We have assume the attenuation for pure water is the result of viscous effects as shown in equation 1. We then transform the attenuation to an effective mechanical Q of the elastic stiffneess [McSkimmin 1964] and then to a complex velocity as shown in Table 3. The addition of 10 % by weight of rock powder Johnson Space Center (JSC1) mars simulant seived to dimensions less than 150 microns and the attenuation due to viscous damping on the cavity walls was assumed to increase the attenuation by a factor of at least 10. We have investigated the heating due to the increase in the attenuation from pure water to attenuation coefficients that are 3 orders of magnitude higher. The attenuation of pure water is of the order o 0.87 dB/m at 1.65 MHz. which

corespondes to a mechanical Q at 1.65 MHz of 10000. Recent calculations by [Hahn and Dual 2015] that the actual attenuation in these systems can be three orders of magnitude higher than the bulk attenuation.

Table 3. The acoustic properties of the borosilicate glass and water and geometry. The baseline attenuation was calculated from equation 1 and converted to mechanical Q =$Re(c^D_{33})/Im(c^D_{33})$ using the transforms outlined by [McSkimin 1964].

Borosilicate Glass
$\rho(kg/m^3) = 2230$
$t_1 = 0.002$, $t_2 = 0.005$, Diameter = 0.0138
$\mathbf{c}^D_{33}$ (x 10^{10} N/m^2) = 7.3 (1 + 0.001i)
$\mathbf{v}_D$ (m/s) = 5703 (1 + 0.0005i)
$\mathbf{\Gamma}/\omega$ (x10^{-4} s/m) = 1.75 (1 – 0.0005i)
Water
$\rho(kg/m^3) = 1000$
t= 0.003, Diameter = 0.0138
$\mathbf{c}^D_{33}$ (x 10^{11} N/m^2) = 2.24 (1 + 0.0001i)
$\mathbf{v}_D$ (m/s) = 1497 (1 + 0.00005i)
$\mathbf{\Gamma}/\omega$ (x10^{-4} s/m) = 6.68 (1 – 0.0005i)

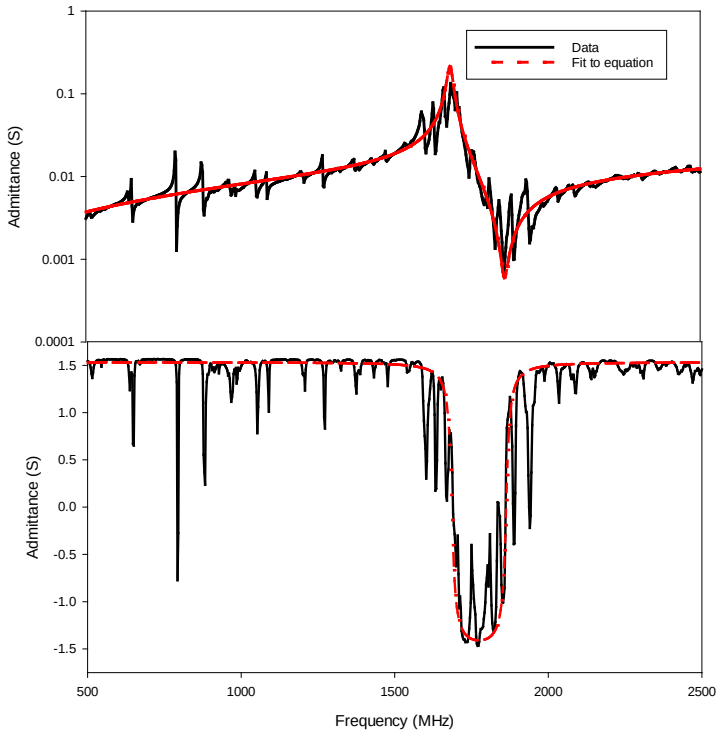

Figure 4. The impedance spectra for the piezoelectric transducer (APC Nebulizer disk # 50-1014) and the fit to the data using the thickness mode impedance equation. The coefficients determined from the fit are shown in Table 2. A variety of radial sideband resonances are clearly present in the spectra.

In order to proceed with the modeling we used the baseline attenuation the water and adjusted the attenuation to determine the heat generation as a function of increased acoustic loss. For a 3 mm thick SCWE chamber between a 2 mm glass on the piezoelectric surface and a 5 mm thick borosilicate cover plate the admittance spectra or the real dissapated power per volt is shown in Figure 5 along with the power dissipated per volt for the bare piezoelectric

transducer. The total power per volt is $P = V^2Y$. For a 1 volt signal $P = (1)^2Y = Y$ and the dissipated power is the real part of this total power. To extrapolate to higher drive voltages multiply by V^2. For example a 10 volt drive signal would produce 100 times the power shown in Figure 5. We have also plotted the admittance (0.02 S) for the output impedance of the amplifier (50 Ohms). Above 0.02 S the amplifier will become burdened and the delivered power will be lower than expected. We can calculate the approximate power required to heat the chamber to achieve 200 ^oC by asumming the heat convection on the top and botton surface area is the dominant heat flow. $Q = hA\Delta T$. If h is 30 W/m^2K and $\Delta T = 175K$ the heat flow for the SCWE chamber area is $Q = P = 1.6$ Watts.

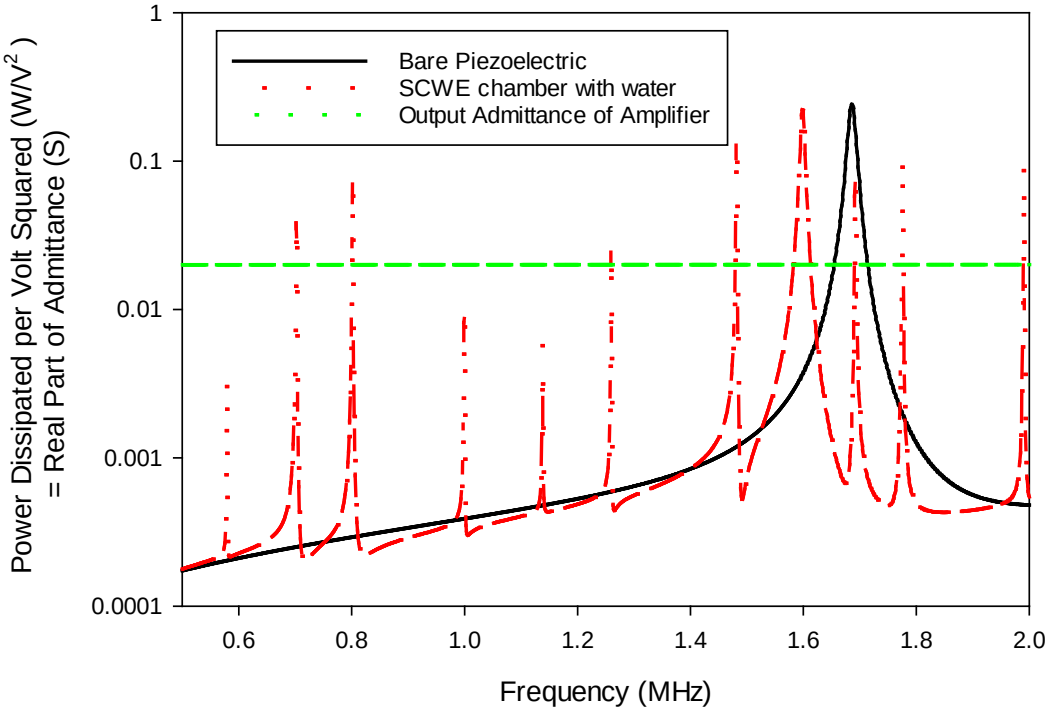

Figure 5. The real part of the admitance spectra or Power per volt squared for the SCWE chamber with diameter D =0.0138, Piezoelectric thickness = 1.23mm, glass thickness = 2mm, Water thickness =3 mm and glass cover plate thickness = 5 mm (blue) compared to the free standing piezoelectric disk resonance (red). The baseline attenuation of water was used. The green line is the load impedance for the amplifier (50 Ohms)

The power dissipated for the same SCWE design but with an increased attenuation (100x) to model the slurry in the water as a function of frequency is shown in Figure 6. The data shown in Figure 5 and 6 are at room temperature. As the SCWE chamber is driven the system is heated and the resonances shift downward due to softening of the glass and piezoelectric. In addition the viscosity of the water is reduced therefore as the slurry is heated one would expect the peaks to become sharper. In order to maintain heating one must track the frequency to make sure that the system is still driven at resonance. The resonances found in Figures 5 and 6 are associated the acoustics of the composite SCWE structure. These are all thickness extensional modes as the network model does not consider mode conversion. The spectra shows the same peeks at low frequency down to 220 kHz and up to 2 MHz however the amplitude of the peak power for each of the resonance is reduced due to the increased damping and the width of the peaks has increased. It should be noted that increasing the temperature of the water to 200 ^oC in a closed container produces very large stresses due to the thermal expansion and incompressibility of water. In the current designs we have injected a gas bubble to act as an expansion volume and to force the pressure to be in equilibrium with the vapor pressure. Even under these reduced pressure condition we have fractured SCWE chambers. This has led to a variety of design iterations to increase the structural integrity of the SCWE chip.

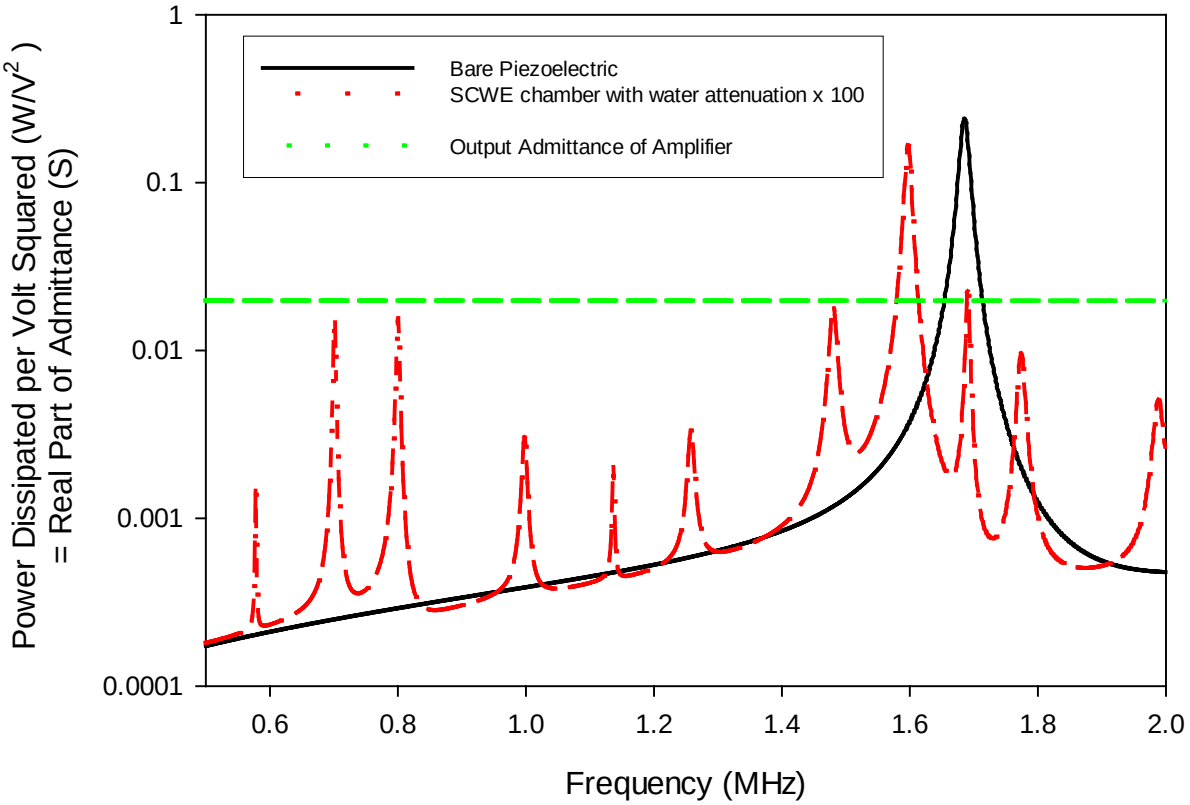

Figure 6. The power dissipation spectra for the SCWE chamber (blue) with diameter D =0.0138, piezoelectric thickness = 1.23mm, glass thickness = 2mm, Water thickness =3 mm and glass cover plate thickness = 5 mm compared to the free standing piezoelectric disk resonance (red). The baseline attenuation of slurry was assumed to be 100x pure water. The green line is the recommended load impedance for the amplifier.

Acoustic SCWE Performance Test Results

An initial SCWE chamber was designed fabricated and tested and is shown in Figure 7 along with a temperature profile of the run. The chip has a Peltier cooler on the top and the bottom of the chip above and below the inlet and outlet of the SCWE chamber to act as freeze valves. A fan is used to cool the hot side of the Peltier cooler on the top cooler to increase the cooling efficiency. The slurry is mixed off chip in an acoustic mixing chamber and is then pumped into the SCWE chamber. The power to the Peltier coolers is applied and the SCWE chamber is sealed. The piezoelectric disk (APC disk # 50-1014) was initially driven by the nebulizer circuit at 1.65 MHz and significant heating was generated however in order to study the various heating regimes we used a Sony Function generator (AFG 320) and an ENI power amplifier (A150 RF – 0.3 -35 MHz) to drive the piezoelectric at frequencies other than the free piezoelectric resonance. The heating curve at 4 frequencies and for a repeated frequency sweep is shown in Figure 7. The data shows discrete frequencies where the power is dissipated into the SCWE chamber as heat. In addition at some frequencies movement of the particles in the slurry was evident. For this particular chip the fastest heating rate was found at 483 kHz. In latter designs at higher temperatures frequencies at 1.82 MHz were found to produce continual heating up to and above 150 ^{o}C. An initial SCWE prototype with geometry similar to the model above (smaller diameter SCWE chamber 12 mm) was tested up to 150 ^{o}C. Structural problems with the design limited the temperature to about 164 ^{o}C before the glass diaphragm would fracture. The initial setup and the heating curves for a 150 ^{o}C run are shown in Figure 8. A series of extractions were completed with this chip at temperatures up to

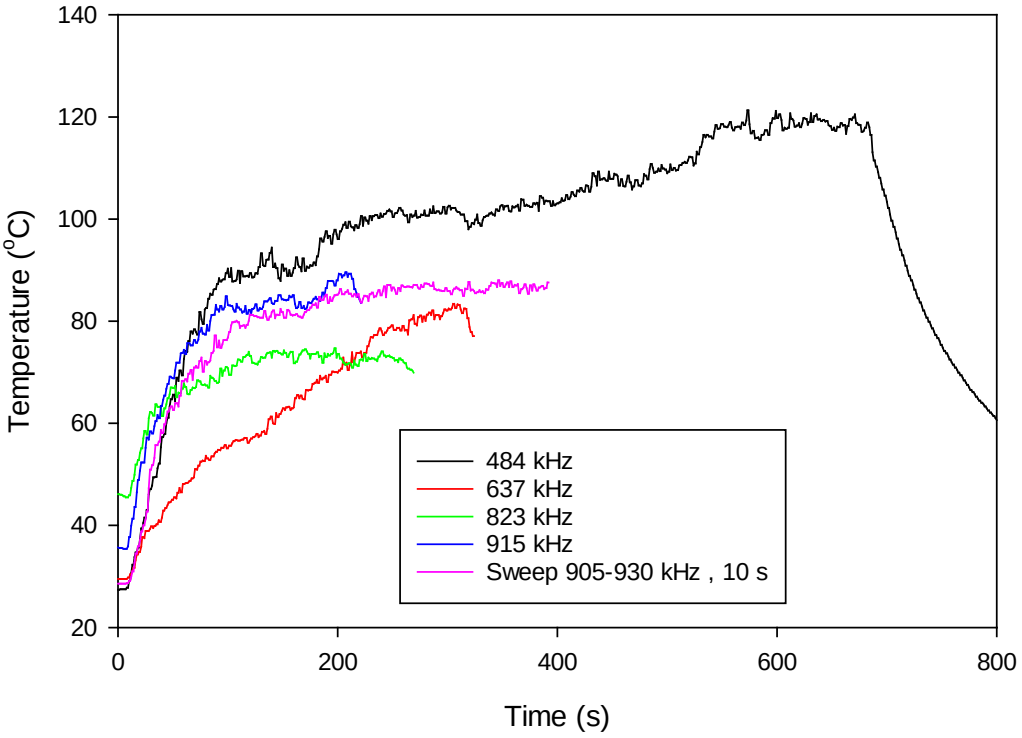

Figure 7. The temperature time profiles at various frequencies and for a repetetive frequency sweep.

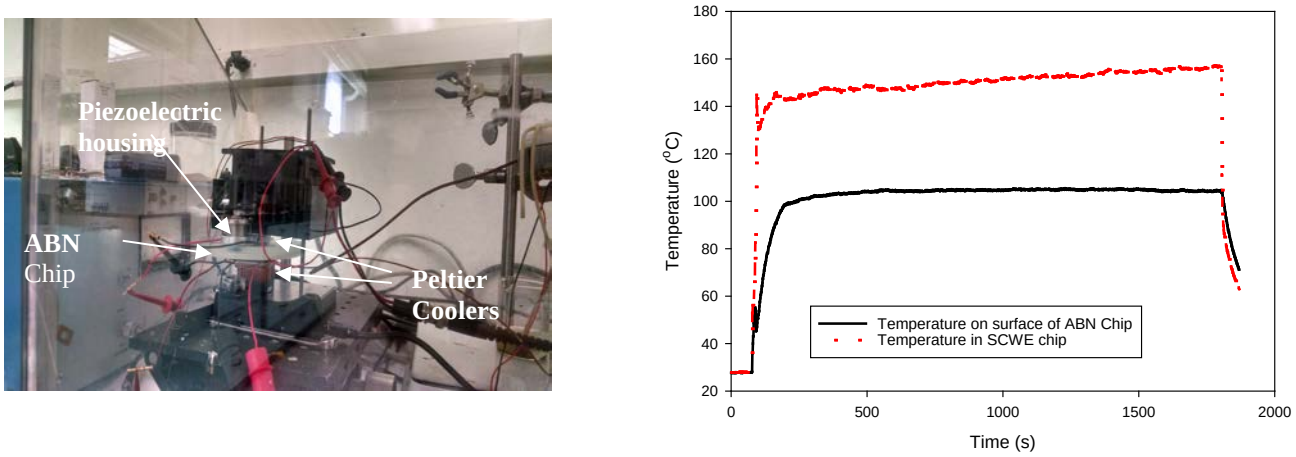

Figure 8. A photograph of the initial experimental apparatus and a curve showing the temperature profile inside the SCWE chamber and on the top surface.

150 °C. In order to increase the maximum temperature in the SCWE chip we re-designed the chip to increase theoretical burst pressure by creating a meandering path above the chip and thereby reducing the effective diaphragm dimension in one dimension. The design change also allowed for more effective flushing of the slurry. In the original open chamber design, vortexes would form and create a dead flow region between the inlet and outlet of the SCWE chamber. The meandering path increased the system was tested and the new test bed and the temperature profile are shown in Figure 9. This device was cycled up to 200°C for > ten minutes five times. After the 5th cycle a fracture in the chip was discovered. In order to increase the reliability of these devices we sought the help of material and structural experts and a variety ideas were generated to potentially increase the device structural integrity and potential the temperature. These included: more refined manufacturing to reduce the critical flaw size, and changing the chip

material from borosilicate to Zerodur®. Other ideas that we have also considered is the preloading the structure to reduce tension forces or switching to a ceramic material with reduced thermal expansion and increased toughness.

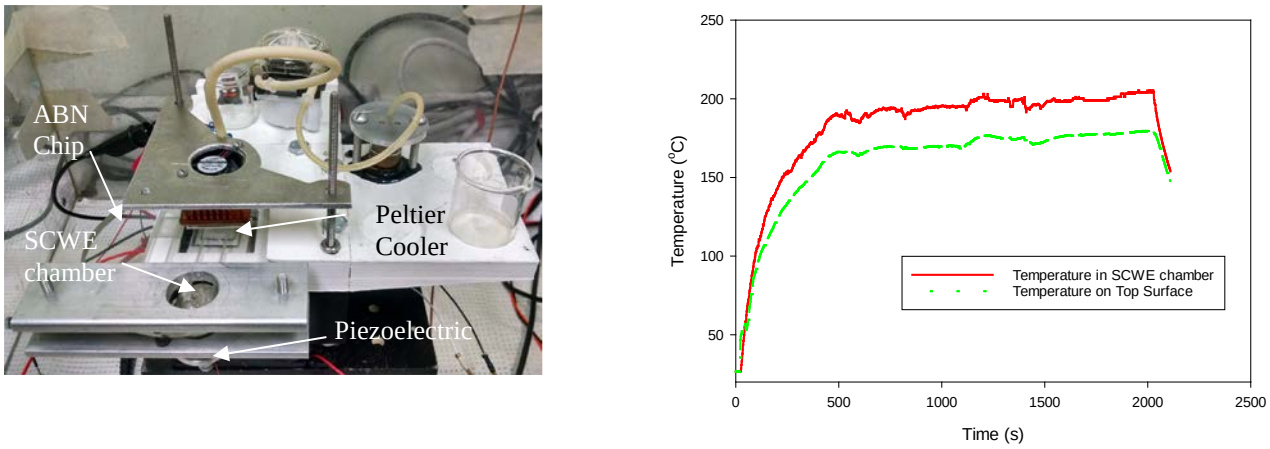

Figure 9. A photograph of the latest experimental apparatus and a curve showing the temperature profile inside and on the top surface of the SCWE chamber. This chip was cycled to 200ºC five times.

Conclusion and Future work

This paper described the modeling and experimentation on the use of a microfluidic acoustic resonant SCWE chamber which is the front end of an amino acid detection instrument called Astrobionibbler. We used Mason's equivalent network model the resonances in the structure including the SCWE fluid chamber. Acoustic pressures excited by a piezoelectric were used to excite a fluid-solid fines mixture in different frequency/amplitude regimes to accomplish a variety of sample processing tasks. To induce heating, the piezoelectric transducer and chamber were driven at high amplitude in resonance. The SCWE chamber with a mixture of water and solid/fines is modelled as acoustic transmission line with a variable loss component. In this regime, heat is pumped into the solution/fines mixture and rapidly heats the sample. In order to assess the validity of the model we have built and tested a variety of chambers. This experimental results which are in general agreement with theory have shown that it is technically feasible to acoustically heat up a solution of water and fines (JSC1 – Mars Simulant sieved to 150 microns) to 200º C. In the acoustic SCWE system a bubble is inserted into the slurry to act as an expansion volume. This bubble keeps the pressure in the SCWE in equilibrium with the vapor pressure of the water and as the temperature increases the pressures can reach up to 16 atmospheres at 200 ºC. The current device is limited by thermal and structural deficiencies however we believe that these can be overcome by appropriate choice of materials, finer machining, and the application of pre-stress.

ACKNOWLEDGMENT

The authors would like to thank Bryan McEnerney and Gary Wang for useful discussions and Michael H. New for funding this work under the Roses ASTID program. The research at the Jet Propulsion Laboratory (JPL), a division of the California Institute of Technology, was carried out under a contract with the National Aeronautics Space Agency (NASA). Reference herein to any specific commercial product, process, or service by trade name, trademark, manufacturer, or otherwise, does not constitute or imply its endorsement by the United States Government or the Jet Propulsion Laboratory, California Institute of Technology.

REFERENCES

A.C. Noell, M. C. Lee, A. M. Stockton, N. Takano, D. Elleman, J. Hasenoehrl, S. Sherrit, F. Grunthaner, (2014) "Astrobionibbler: Microfluidic Subcritical Water Extraction Of Organics From Planetary Samples ", 2nd International Conference on MicroFluidic Handling Systems October 8-10, University of Freiburg, Germany

A.C. Noell, A.M. Fisher, N. Takano, M. C. Lee, J. Hasenoehrl, S. Sherrit, F. Grunthaner, (2015) "Astrobionibbler: Microfluidic Subcritical Water Extraction Of Organics on Mars", #7389, Astrobiology Science Conference June 15 – 19, Chicago, IL.

Amashukeli, X., Pelletier, C. C., Kirby, J. P., & Grunthaner, F. J. (2007). Subcritical water extraction of amino acids from Atacama Desert soils. *Journal of Geophysical Research: Biogeosciences*, *112*(G4).

Bao, X., Bar-Cohen, Y., Sherrit, S., Badescu, M., & Louyeh, S. (2009, March). Transport powder and liquid samples by surface acoustic waves. In *SPIE Smart Structures and Materials+ Nondestructive Evaluation and Health Monitoring* (pp. 72910M-72910M). International Society for Optics and Photonics.

Benthin, B., Danz, H., & Hamburger, M. (1999). Pressurized liquid extraction of medicinal plants. *Journal of Chromatography A*, *837*(1), 211-219.

Berlincourt, D. A., Curran, D.R., Jaffe, H., (1964) "Chapter 3- Piezoelectric and Piezomagnetic Material and their Function in Transducers, pp. 169-270, Physical Acoustics- *Principles and Methods*, Volume 1-Part A, ed. W.P. Mason Academic Press, New York

Bruus, H., Dual, J., Hawkes, J., Hill, M., Laurell, T., Nilsson, J., ... & Wiklund, M. (2011). Forthcoming Lab on a Chip tutorial series on acoustofluidics: Acoustofluidics—exploiting ultrasonic standing wave forces and acoustic streaming in microfluidic systems for cell and particle manipulation. *Lab on a Chip*, *11*(21), 3579-3580.

Carabias-Martínez, R., Rodríguez-Gonzalo, E., Revilla-Ruiz, P., & Hernández-Méndez, J. (2005). Pressurized liquid extraction in the analysis of food and biological samples. *Journal of Chromatography A*, *1089*(1), 1-17.

Glynne-Jones, Peter, Boltryk, Rosemary J. and Hill, Martyn, 2012, " Acoustofluidics 9: Modeling and applications of planar resonant devices for acoustic particle manipulation", Lab Chip, 2012, 12, 1417

Hahn, P., & Dual, J. (2015). A numerically efficient damping model for acoustic resonances in microfluidic cavities. *Physics of Fluids (1994-present)*, *27*(6), 062005.

Hawthorne, S. B., Grabanski, C. B., Martin, E., & Miller, D. J. (2000). Comparisons of Soxhlet extraction, pressurized liquid extraction, supercritical fluid extraction and subcritical water extraction for environmental solids: recovery, selectivity and effects on sample matrix. *Journal of Chromatography A*, *892*(1), 421-433.

King, L. V. (1934, November). On the acoustic radiation pressure on spheres. In *Proceedings of the Royal Society of London A: Mathematical, Physical and Engineering Sciences* (Vol. 147, No. 861, pp. 212-240). The Royal Society.

Liang, X., & Fan, Q. (2013). Application of sub-critical water extraction in pharmaceutical industry. *Journal of Materials Science and Chemical Engineering*, *1*(05), 1.

M Chaplin, (2015), Water Structure and Science, http://www1.lsbu.ac.uk/water/ [Downloaded Dec 30 2015]

Miller, S. L. (1953). A production of amino acids under possible primitive earth conditions. Science, 117(3046), 528-529.

Mason W..P.(1948), Electromechanical Transducers and Wave Filters, Princeton, NJ, Van Nostrand

Mason W..P.(1958), Physical Acoustics and the Properties of Solids, D. Van Nostrand Co., Princeton, NJ

McSkimin, H. J. (1964). Ultrasonic methods for measuring the mechanical properties of liquids and solids. *Physical Acoustics*, *1*(part A), 271-334.

Ramos, L., Kristenson, E. M., & Brinkman, U. T. (2002). Current use of pressurised liquid extraction and subcritical water extraction in environmental analysis. *Journal of Chromatography A*, *975*(1), 3-29.

Saim, N. A., Dean, J. R., Abdullah, M. P., & Zakaria, Z. (1997). Extraction of polycyclic aromatic hydrocarbons from contaminated soil using Soxhlet extraction, pressurised and atmospheric microwave-assisted extraction, supercritical fluid extraction and accelerated solvent extraction. *Journal of Chromatography A, 791*(1), 361-366.

Sherrit, S., Leary, S. P., Dolgin, B. P., & Bar-Cohen, Y. (1999). Comparison of the Mason and KLM equivalent circuits for piezoelectric resonators in the thickness mode. In *Ultrasonics Symposium, 1999. Proceedings. 1999 IEEE* (Vol. 2, pp. 921-926). IEEE.

Yanik, J., Yüksel, M., Sağlam, M., Olukçu, N., Bartle, K., & Frere, B. (1995). Characterization of the oil fractions of shale oil obtained by pyrolysis and supercritical water extraction. *Fuel*, *74*(1), 46-50.
Hamdan, S., Daood, H. G., Toth-Markus, M., & Illés, V. (2008). Extraction of cardamom oil by supercritical carbon dioxide and sub-critical propane. *The Journal of Supercritical Fluids*, *44*(1), 25-30.

Yang, Y., Bowadt, S., Hawthorne, S. B., & Miller, D. J. (1995). Subcritical water extraction of polychlorinated biphenyls from soil and sediment. *Analytical Chemistry*, *67*(24), 4571-4576.

Yosioka, K., & Kawasima, Y. (1955). Acoustic radiation pressure on a compressible sphere. *Acta Acustica united with Acustica*, *5*(3), 167-173.